



Research paper

Assessing the involvement of tumor-secreted factors in the inhibition of muscle differentiation

Miranda van der Ende^{a,b,1}, Xiaolin Li^{a,1}, Mieke Poland^a, Fleur Jansen^a, Jocelijan Meijerink^a, Jaap Keijer^b, Renger F. Witkamp^a, Sander Grefte^b, Klaske van Norren^{a,*}

^a Division of Human Nutrition and Health, Wageningen University, Wageningen, the Netherlands

^b Human and Animal Physiology, Wageningen University, Wageningen, the Netherlands



ARTICLE INFO

Keywords:

Muscle wasting
Cancer cachexia
Cytokines
Creatine kinase
PGE2
C2C12 cells

ABSTRACT

Cancer cachexia is a multifactorial syndrome characterized by involuntary and pathological weight loss, predominantly caused by muscle wasting. While tumors can elicit detrimental effects on skeletal muscle function, the contribution of specific tumor-derived mediators remains elusive. To explore this, we investigated the impact of conditioned media (CM) from four cachexia-inducing tumor cell lines (KPC, 4662, LLC, and C26) on muscle differentiation using C2C12 cells. Creatine kinase (CK) activity was measured as an indicator of muscle wasting, and global gene expression changes in C2C12 cells were analyzed via RNA sequencing. Cytokine profiling of the CM identified 111 immune factors, and mimic combinations of the most abundant cytokines from KPC CM were tested for their effects on CK activity. Additionally, the involvement of tumor-derived PGE2 was assessed via CRISPR/Cas9-mediated knockout of the *Ptgs2* gene in KPC cells. CM from all tumor cell lines significantly reduced CK activity in C2C12 cells, consistent with downregulation of *CKm* gene expression. Global gene expression profiles revealed upregulation of immune-related pathways in C2C12 cells exposed to KPC CM. However, mixtures of the 14 most abundant cytokines in CM had minimal effects on CK activity, and tumor-derived PGE2 showed no significant effect on CK activity or muscle cell differentiation. These findings suggest that the observed muscle-wasting effects of cachexia-inducing tumor cells cannot be replicated by the most abundant cytokines present in CM alone, highlighting the need for further research to identify the key tumor-derived factors responsible for cancer-induced muscle wasting.

1. Introduction

Over 80 % of cancer patients experience cachexia, which is characterized by loss of skeletal muscle mass, with or without loss of fat mass [1,2]. In Europe, about half of colorectal cancer patients develop cachexia [3–5], while 80–90 % of lung and pancreas cancer patients are at risk for the syndrome [6]. Unfortunately, effective treatment of cachexia is still lacking [7]. The loss of skeletal muscle mass is caused by different processes within the muscle itself: 1) an imbalance between protein synthesis and breakdown; 2) structural remodeling of the myofiber (from type I to type II muscle fibers); 3) impaired muscle degeneration and regeneration; and 4) alteration in mitochondrial functioning [8]. Consequently, myogenesis, the formation of skeletal muscular tissue, is inhibited during cancer cachexia [9]. Recent findings also suggest that decreased skeletal muscle regeneration plays a role in the

development of cachexia [10]. However, little is known about the mechanisms by which cancer cells affect skeletal muscle regeneration, particularly in the context of injury or stress, which is clinically relevant in cachectic patients undergoing surgery, trauma, or falls [11,12]. Prior studies have mainly focused on atrophy of mature myotubes, whereas the impact on muscle regeneration after injury or minor stress remains underexplored. Satellite cells, the key mediators of regeneration, often fail to properly fuse with muscle fibers in cachexia, despite upregulation of early myogenic markers such as Pax7 and MyoD/Pax3, indicating an attempted regenerative response [12–15]. A paper by Guttridge et al. indicates a role for soluble factors excreted by the tumor [16].

A range of tumor-secreted factors that influence muscle catabolism have been identified. For example, insulin-like growth factor binding protein 3 (IGFBP3), C-X-C motif chemokine ligand 1 (CXCL1), and C–C motif chemokine ligand 2 (CCL2) have been found to reduce the number

* Corresponding author.

E-mail address: klaske.vannorren@wur.nl (K. van Norren).

¹ These authors contributed equally to this work.

of nuclei per myotube in C2C12 cells [17]. Additionally, studies showed that IGFBP3 derived from pancreatic cancer cells, at concentrations ranging from 0.1 to 5 $\mu\text{g}/\text{mL}$, decreases myogenesis in C2C12 cells [18]. These findings indicate that tumor-derived factors can directly interfere with myoblast differentiation and impair the early stages of muscle regeneration. Furthermore, prostaglandin E2 (PGE2), associated with tumor growth and development [19], has also been shown to upregulate the expression of both interleukin 6 (IL6) and tripartite motif containing 63 (TRIM63) [20]. Conversely, certain prostaglandins, such as prostaglandin F2 alpha (PGF2 α), are hypothesized to stimulate the growth of skeletal muscle cells [21]. Collectively, these studies suggest that tumor-secreted factors can directly disrupt muscle regenerative processes in addition to promoting muscle wasting, highlighting the dual impact of cancer on muscle tissue. However, it is important to note that these studies have not performed comprehensive screenings and did not consider the actual concentrations of tumor-derived factors observed in conditioned media of tumor cells.

To further elucidate the direct influence of cancer cells on muscle, we employed an in vitro approach by exposing skeletal muscle cells to conditioned medium (CM) from cell lines that are known to induce cachexia in vivo. The pancreatic ductal adenocarcinoma-derived cell lines (KPC and 4662) [22,23] are both inducing cachexia in vivo and are commonly used to study cancer-induced cachexia. Additionally, we employed the Lewis lung carcinoma (LLC) cell line along with the colon 26 carcinoma (C26) cell line [24,25] to investigate the impact of cancer-induced cachexia. Murine C2C12 myoblasts, which can be differentiated into myotubes, were used as an in vitro model of skeletal muscle tissue.

Importantly, by exposing C2C12 cells during differentiation, we specifically model how tumor-derived factors interfere with myoblast differentiation and early regenerative processes, rather than simply inducing atrophy in fully formed myotubes. This approach provides a relevant platform to study the mechanisms by which cancer affects muscle repair, which is critical for understanding delayed recovery in cachectic patients following injury. Evaluation parameters include the quantification of myotube nuclei, measurement of myotube diameter, and the assessment of expression of key myogenesis markers or creatine kinase (CK) activity. Creatine kinase, crucial for regulating cellular adenosine triphosphate (ATP) concentration, exhibits elevated levels in cells with high ATP demands [26].

In our study, we focused on the influence of tumor secretions and immune factors on the parameters of C2C12 muscle myogenesis. We first assessed the impact of conditioned media (CM) from four cancer cachexia-inducing cell lines (KPC, 4662, LLC, and C26) on myogenesis by measuring CK activity. We then generated a CRISPR/Cas9-mediated *Ptgs2* gene knockout in the KPC cancer cells to study the involvement of cyclooxygenase-2 (COX2) and its major product PGE2, as previously suggested [27]. Next, we conducted RNA sequencing of differentiating C2C12 cells exposed to CM to identify prominently regulatory processes. Based on the outcome, we established profiles of soluble immune modulators in the CM and made different mixtures (mimics) in cell culture medium. The effects of these mimics on C2C12 cells were then assessed.

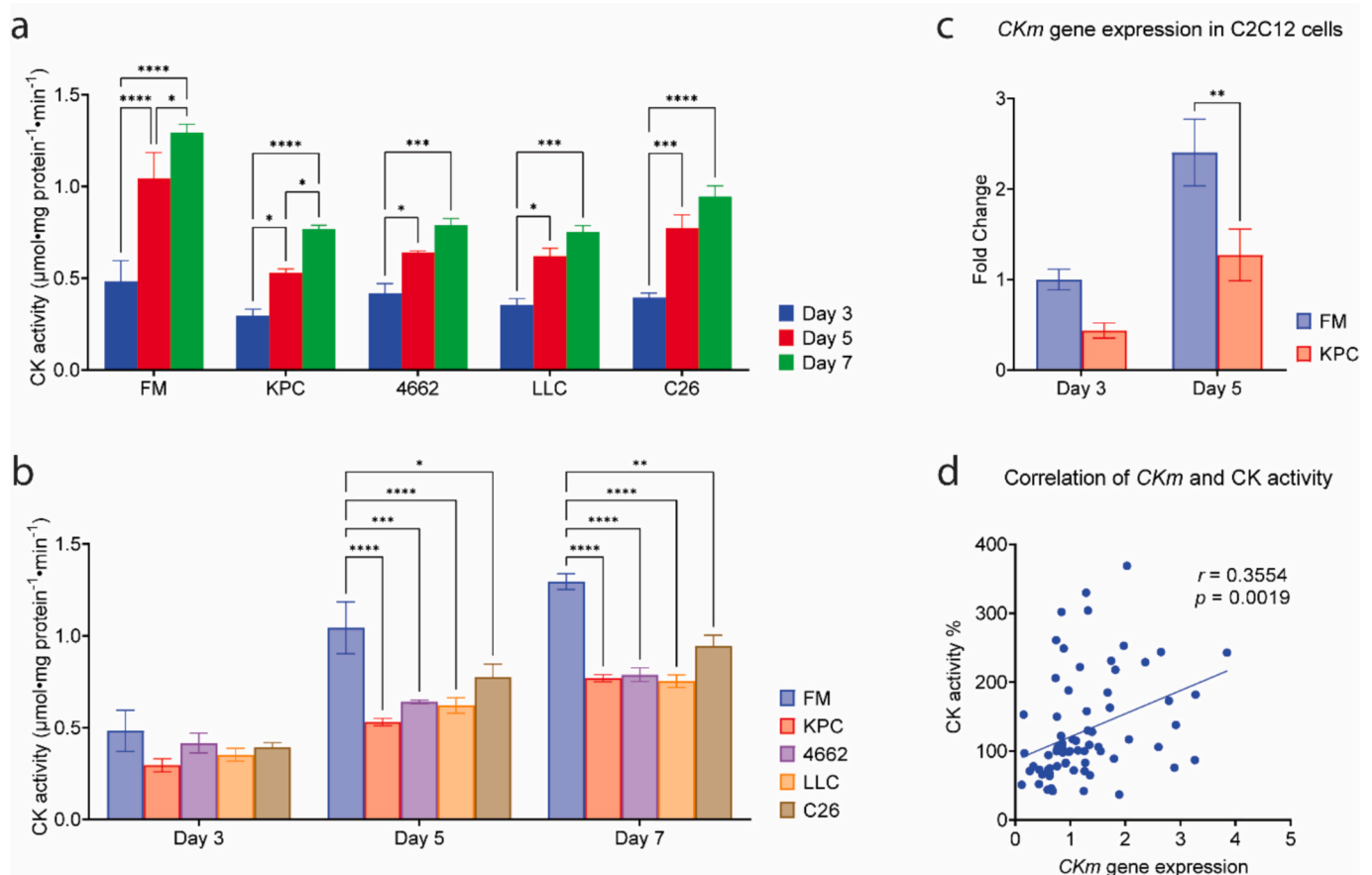


Fig. 1. Media of cachexia-inducing tumor cells decrease CK activity and *CKm* gene expression in C2C12 cells. **a** and **b** CK activity in differentiating C2C12 cells exposed to cachexia-inducing tumor media on day 3, day 5, and day 7. $N = 3$ (triplicate per N). **c** qPCR of *CKm* in differentiating C2C12 cells exposed to KPC CM on day 3 and day 5. $N = 7$ (duplicate or triplicate per N). **d** Pearson correlation of CK activity (% of FM control) and *CKm* gene expression. All data were expressed as mean \pm SEM. Data represented in **a**, **b**, and **c** were analyzed by two-way ANOVA with Bonferroni's post hoc test. **d** Analyzed by simple linear regression and two-tailed correlation analyses. * $p \leq 0.05$, ** $p \leq 0.01$, *** $p \leq 0.001$, and **** $p \leq 0.0001$.

2. Results

2.1. Media of cachexia-inducing tumor cells decrease CK activity and CKm gene expression in C2C12 cells

Differentiating C2C12 cells were exposed to CM to evaluate their effects on CK activity. To rectify nutrient depletion within the CM, a 33 % dilution was employed using fresh medium (FM). Upon incubation with CM of KPC, 4662, C26, and LLC, CK activity increased slowly with time in C2C12 cells (Fig. 1a) but remained significantly lower than the FM control group on day 5 and day 7 during differentiation (Fig. 1b). No time- (days of differentiation) or interaction effects were found, which precludes testing the significance on specific days. The CM of KPC cells induced a pronounced change in CK activity compared to the FM group (day 5: 0.53 vs. 1.04 $\mu\text{mol}/\text{mg}$ protein/min, $P < 0.0001$; day 7: 0.77 vs. 1.30 $\mu\text{mol}/\text{mg}$ protein/min, $P < 0.0001$). To validate the observed changes in CK activity, gene expression of *CKm* in C2C12 cells incubated with KPC CM was analyzed. Significant downregulation ($P < 0.01$) of *CKm* was observed on day 5 (Fig. 1c). With the most pronounced effects on CK activity observed on days 3 and day 5, these timepoints were selected to determine *CKm* gene expression. Additionally, we observed a positive correlation between CK activity (% of FM control) and *CKm* gene expression (Pearson $r = 0.3554$ and $P = 0.0019$) based on results from both day 3 and day 5 (Fig. 1d). These findings indicate that exposure to CM results in a reduction of both CK activity and *CKm* gene expression in C2C12 cells. In addition, at day 3 and 5 of C2C12 differentiation, KPC CM induced a reduction in the expression of most myosin heavy chain (MyHC) genes (Supplemental Fig. 1), reflecting impaired myogenesis in C2C12 cells.

2.2. Immune-related processes in C2C12 are activated after CM incubation

Subsequently, we performed a comprehensive gene expression analysis on C2C12 cells exposed to all conditioned media. RNA was extracted from C2C12 cells on differentiation days 3 and 5. The normalized gene expression profiles of the samples were analyzed using principal component analysis (PCA) (Fig. 2a). In PC1, explaining 55 % of the variance, a clear distinction was observed between the samples harvested on day 3 and on day 5, confirming differences in response between these days. PC2 explains 18 % of the variance, which is mainly due to the differences between the experiments (batch difference). The whole dataset consisted of 23,169 different genes, and the number of differentially expressed genes (DEGs) per cell line was calculated. The CM of all tested cachexia-inducing cell lines provoked gene expression responses in the C2C12 cells; the KPC and LLC CM exposures showed the most DEGs on both day 3 and day 5, while C26 CM induced the smallest differential effect. For all cell lines, more DEGs were found on day 5 of C2C12 differentiation than on day 3.

To better understand how soluble mediators in CM affect muscle cells, the Gene Ontology (GO) terms in Biological Process (BP) related to the gene expression profiles on day 5 were analyzed (Fig. 2b). Of the significant top 20 upregulated and the top 20 downregulated GO terms, exposure of C2C12 cells to the CM of the 4662 cells resulted in the highest significant regulated GO terms (total of 32 out of 40) and incubation with C26 CM in the lowest number (total of 5 out of 40). Among the upregulated GO terms, most were related to immune processes. Six GO terms were related to leukocyte migration, and other terms were related to responses to an external stimulus, bacterium, and virus. The only GO term that was commonly, and highly significantly, upregulated in all CM conditions was 'cytokine-mediated signaling pathway'. The downregulated GO terms revealed a distinct pattern, primarily associated with skeletal muscle and mitochondrial functions, notably the electron transport chain. The most significant downregulation was observed in cells exposed to CM of the 4662 cell line, particularly the 'rRNA metabolic processes'. Overall, downregulated

pathways were mainly related to muscle wasting, while upregulated pathways suggest a potential role for cytokines or immune factors as inducers. Based on these results, we further focused on immune signals as potential inducers of cachexia.

In addition, we examined the expression of myosin heavy chain (MyHC) isoforms as stage-specific markers of myogenic differentiation (Fig. 3). KPC CM significantly reduced *Myh3* at day 3, an early developmental isoform, and suppressed *Myh1*, *Myh2*, and *Myh7* at day 5, which are characteristic of later differentiation and maturation. In contrast, C26 and 4662 CM did not significantly alter any MyHC isoforms, while LLC CM exhibited only minor effects. These findings indicate that tumor-derived factors exert cell line-specific effects on myogenesis, with KPC CM in particular impairing both early and late stages of the differentiation program.

2.3. Assessment of tumor-derived immune factors influencing C2C12 cell differentiation

Since RNA expression profiles pointed in the direction of cytokines and immune factors driving reduced C2C12 differentiation, and since cytokines have been implicated in muscle wasting [17,28], we subsequently analyzed inflammatory signaling-related gene expression in C2C12 cells exposed to CM and predicted possible upstream regulatory factors (Fig. 4a). $\text{TNF}\alpha$ was found to be an upstream regulator in all four CM conditions. Additionally, the following upstream cytokines were found in two conditions: interleukin 1 alpha ($\text{IL1}\alpha$) (KPC and LLC), C-X-C motif chemokine ligand 12 (CXCL12) (KPC and 4662), C-X-C motif chemokine ligand 1 (CX3CL1) (KPC and C26), and SPP1 (4662 and LLC).

Following this prediction from upstream regulatory factors, we investigated which factors were present in the CM at the protein level, potentially explaining the immune response of the C2C12 cells upon exposure to CM. To this end, a cytokine array was used to screen for the presence of 111 different cytokines. Of the 111 cytokines assessed, 75 were not expressed at higher levels than in cells exposed to FM, whereas for 36 cytokines a higher expression was found compared to cells exposed to FM (Supplemental Fig. 1). The relative levels of the cytokines varied between different CMs, except for cystatin C. The most abundant cytokines found were CCL20, MMP3, Insulin-like growth factor-binding protein 6 (IGFBP6), and osteoprotegerin (Supplemental Fig. 1). To assess the potential role of these cytokines in the observed effects on CK activity and gene expression, mimics were generated by mixing cytokines at concentrations reflective of those found in CM. The composition of cytokines and their concentrations present in CM from KPC cells served as the basis for these mimics, as KPC CM evoked the strongest response in C2C12 cells based on DEGs and CK activity. Cytokine array analysis revealed that KPC CM exhibited the highest relative levels of CCL20, CXCL5, PCSK9, CXCL16, VEGF, Serpin E1, IGFBP3, and CXCL1. To determine precise immune factor concentrations for the mimics, levels of these most dominant cytokines were measured across all CMs. Additionally, concentrations of SPP1, $\text{TNF}\alpha$, IL6, CCL2, LIF, and prostaglandins PGE2 and $\text{PGF2}\alpha$ were established based on upstream regulator analysis and literature data (Fig. 4b). Notably, KPC CM contained low levels of IL6 (0.0012 ng/mL), LIF (0.003 ng/mL), whereas $\text{TNF}\alpha$ was not detectable.

Based on these starting points, four immune factor mimics were composed to establish a possible causality. These consisted of: A) CXCL1, VEGF, CXCL16, Serpin E1, CCL20, PCSK9, IGFBP3, and CXCL5; B) PGE2 and $\text{PGF2}\alpha$; C) SPP1, IL6, CCL2, and LIF; D) a combination of A, B and C. C2C12 cells were exposed to all four mimics during differentiation for 3, 5 and 7 days and CK activity was measured and expressed as a percentage of the FM control (Fig. 4c). The KPC CM significantly decreased the CK activity of the C2C12 cells on all differentiation days (56 % on day 3, 65 % on day 5, 68 % on day 7). By contrast, the effects of the mimics were much smaller, and CK activity was restored to 100 % of the FM controls by day 7 of differentiation (Fig. 4c). Only mimic D decreased the overall CK activity on day 3 (69 %, $P < 0.05$), but this

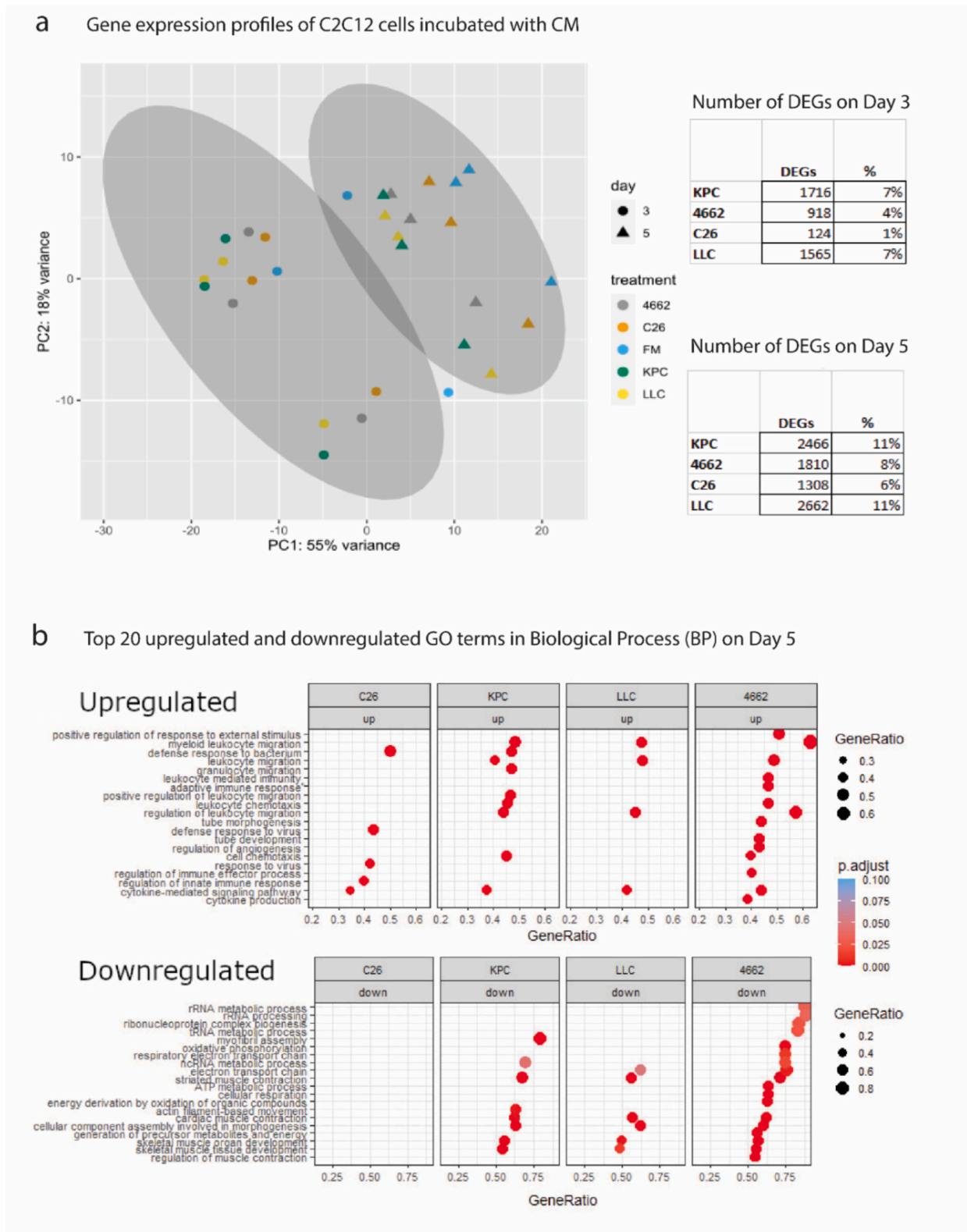


Fig. 2. Immune-related processes in C2C12 cells are activated after CM incubation. a PCA plot of the variation of the normalized differences in RNA expression patterns of C2C12 on differentiation day 3 and day 5, after incubation with different conditioned media of cancer cachexia-inducing cell lines (KPC, 4662, LLC and C26). Number and percentage of DEGs of the total dataset on day 3 and day 5 of C2C12 differentiation with fresh differentiation medium (FM), $N = 3$. b Highest significant top 20 upregulated and downregulated Gene Ontology (GO) terms in Biological Process (BP) on day 5 after incubation of C2C12 with different CM. * = The name of this GO term was shortened, the full name is Adaptive immune response based on somatic recombination of immune receptors built for immunoglobulin superfamily domains.

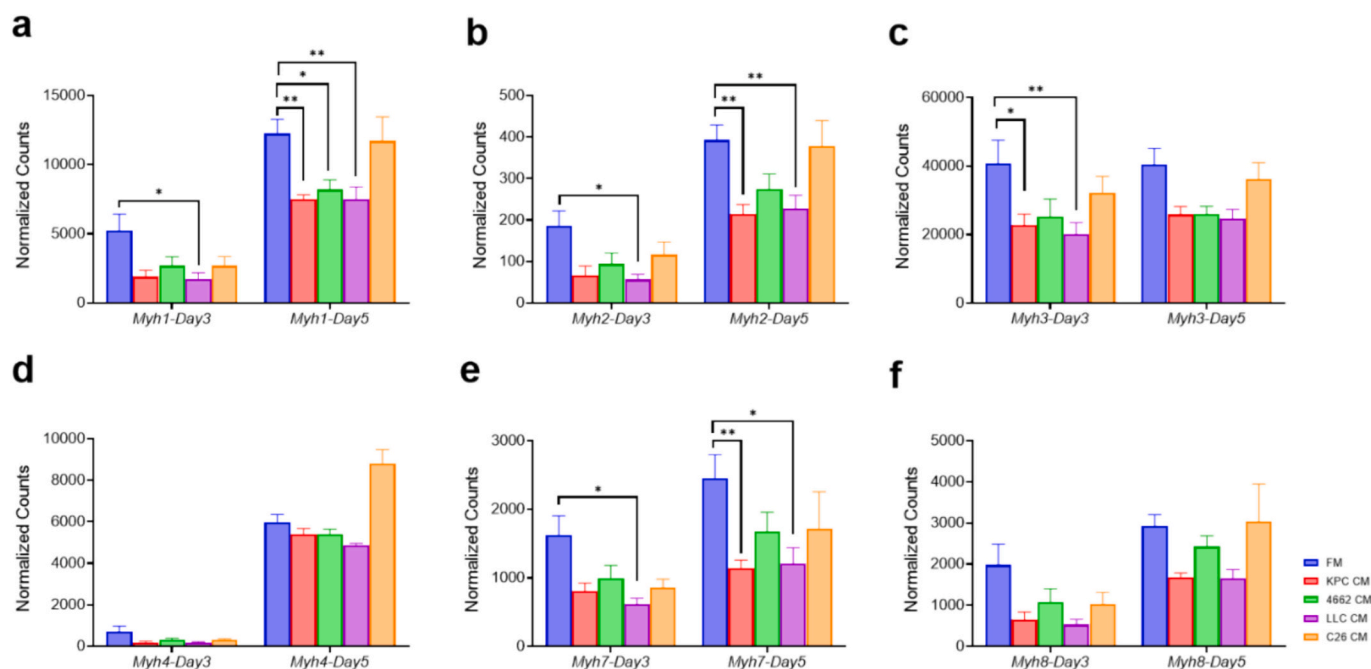


Fig. 3. RNA-seq analysis of myosin heavy chain (MyHC)-related gene expression in C2C12 cells exposed to cachexia-inducing tumor cell media. Normalized counts for **a** *Myh1*, **b** *Myh2*, **c** *Myh3*, **d** *Myh4*, **e** *Myh7*, and **f** *Myh8* in differentiating C2C12 cells exposed to cachexia-inducing tumor media on day 3 and day 5, compared to FM control. N = 3 (triplicates per condition). Data were expressed as mean \pm SEM and were analyzed by two-way ANOVA followed by Dunnett's multiple comparisons test. * $p \leq 0.05$, ** $p \leq 0.01$, *** $p \leq 0.001$, and **** $p \leq 0.0001$.

disappeared at later time points without significant suppression on day 5 and day 7 (Fig. 4d). These results indicate that the 14 tumor-secreted factors identified do not directly influence muscle cell differentiation during the observation period.

2.4. Validating the role of tumor-derived PGE2 on C2C12 cell differentiation

In our previous study, the involvement of tumor-secreted PGE2 and its key producing enzyme COX2 in the multi-organ crosstalk during KPC-induced cachexia was demonstrated [27]. To investigate the influence of PGE2 specifically on C2C12 differentiation, we first measured PGE2 concentrations in the CM of the four cachexia-inducing tumor cell lines (Fig. 5a). PGE2 was indeed found in these secretions, especially in KPC CM (8.67 ng/mL) and C26 CM (30.64 ng/mL) (Fig. 5a). To investigate the role of COX2, we performed CRISPR/Cas9-mediated knockout (KO) of *Ptgs2* (encoding COX2) in the KPC cell line. This knockout of *Ptgs2* resulted in a markedly reduced concentration of PGE2 in the medium (Fig. 5b), in line with a decreased *Ptgs2* gene expression (Fig. 5c). No interference with *Ptgs1* (encoding COX1) gene expression was found in the KPC cells (Fig. 5d).

C2C12 cells exposed to *Ptgs2*-KO CM showed a significantly reduced CK activity compared to the FM group ($P < 0.01$), while they showed no significant change compared to KPC CM (Fig. 5e). For *CKm* gene expression in C2C12 cells exposed to KPC CM and *Ptgs2*-KO CM on day 6, no significant changes were observed compared to the FM control group (Fig. 5f). These data indicate that knocking out COX2 in KPC cells does not restore the inhibitory effect produced by KPC CM on CK activity in C2C12 cells during the observation period.

3. Discussion

Our findings confirm a persistent inhibitory effect of tumor cell secretions on CK activity during in vitro C2C12 muscle differentiation, demonstrating that tumor-derived factors directly impair early myogenic processes and regenerative potential. This suppression is

accompanied by prominent alterations in immune signaling pathways. We further show that a combination of the 14 most abundant cytokines in the CM, partially mimicking tumor-derived secretions, significantly inhibited CK activity at day 3. However, this inhibition is not sustained on days 5 and 7, suggesting the involvement of additional factors. Moreover, knockout of tumor-associated COX2, which leads to a decrease in PGE2 secretion, does not mitigate the negative impact on muscle differentiation.

Cachexia-inducing tumor secretion decreased myogenesis in differentiated C2C12 cells by an average of 4 days when exposed to C26 CM [29–33], LLC CM [33,34], and KPC CM [35,36], as assessed through myotube diameter. A previous study showed that serum from pancreatic cancer patients induced the death of C2C12 cells and primary myoblasts [15], aligning with the effects of KPC CM observed in our study. Importantly, these effects reflect disruption of muscle regeneration rather than simply atrophy of mature myotubes, highlighting the clinical relevance of our model for understanding impaired recovery following injury, surgery, or trauma in cachectic patients. This also captures the physiological contribution of satellite cells, which often fail to fuse with existing fibers in cachexia despite upregulation of early markers like Pax7 and MyoD/Pax3, indicating attempted regeneration. Inflammatory cytokines, such as TNF α , IL6, and IL1 α , are key mediators in this process [28,37–39], as they alter gene expression in myocytes, not only promoting catabolism but also inhibiting myoblast differentiation and fusion, critical steps in muscle repair [40]. Our results underscore that tumor secretions can interfere with the regenerative program of skeletal muscle, providing a mechanistic link between cachexia and impaired muscle regeneration.

In the search for potential mediators, COX2 has frequently emerged as a key player due to its consistent upregulation in tumors. This upregulation leads to increased prostaglandin production, contributing to the heightened inflammatory state often associated with cancer [41,42]. Among prostaglandins, PGE2 is notably produced by various human solid tumors, including those of colon [43,44], lung [45], and pancreatic [46,47] cancer. The role of PGE2 in regulating protein turnover is also known from exercise training adaptations in human muscle [48].

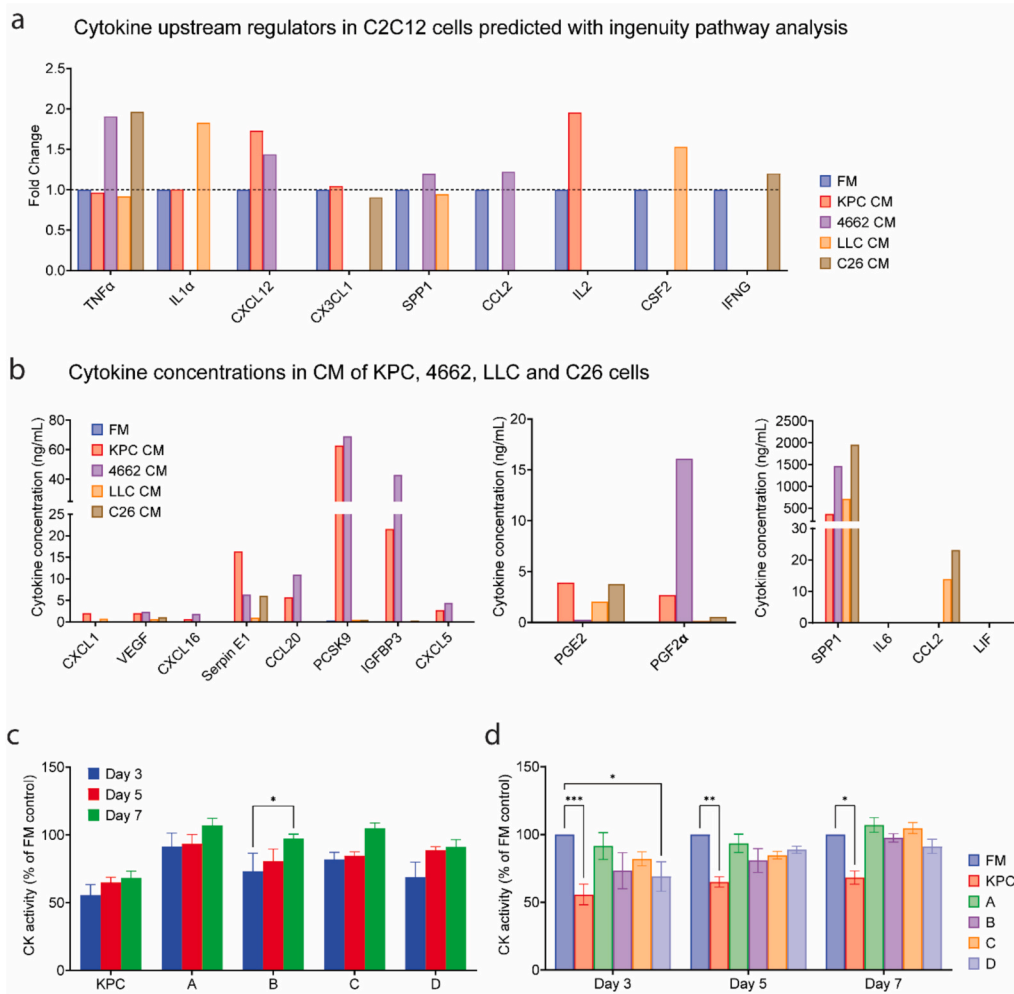


Fig. 4. Assessment of tumor-derived immune factors influencing C2C12 cell differentiation. **a** Cytokine upstream regulators in C2C12 cells identified with Ingenuity Pathway Analysis (IPA) with an activation z-score > 2 and a fold change > 0.9 on day 5 after incubation with different CM. **b** Cytokine concentrations were measured in CM of KPC, 4662, LLC, and C26 cells ($N = 1$). **c** and **d** CK activity in C2C12 cells presents as a percentage of FM control, $N = 4$ (duplicate per N). Data represented in **c** and **d** were expressed as mean \pm SEM and were analyzed by one-way ANOVA with Tukey post hoc test. Significant effects compared to FM are applicable to the three different days within the condition and are represented with * $p \leq 0.05$, ** $p \leq 0.01$, *** $p \leq 0.001$, and **** $p \leq 0.0001$. Immune factor mimics consist of 33 % of measured concentration in KPC CM: (A) CXCL1, VEGF, CXCL16, Serpin E1, CCL20, PCSK9, IGFBP3, and CXCL5; (B) PGE2 and PGF2 α ; (C) SPP1, IL6, CCL2, and LIF; (D) mimic A, B, and C together.

Another prostaglandin, PGF2 α , has been reported to stimulate PI3K/ERK/mTORC1 signaling which results in increased C2C12 myotube diameter [49] while cancer cachexia is known for its downregulation of mTOR expression in muscle [37]. Our previous in vitro study demonstrated that the COX2 inhibitor celecoxib reduced PGE2 formation in tumor cells [27]. Furthermore, our previous study in mice showed that tumor-specific *Ptgs2* gene knockout ameliorated pancreatic cancer cachexia and improved survival. By contrast, the results of the present study do not point in this direction. Neither the conditioned media of COX2 knockout cells nor 'mimic' mixtures containing PGE2 and PGF2 α had a notable impact on C2C12 cell differentiation, although a significant reduced CK activity was seen at day 3 of differentiation. These observations suggest that multiple soluble factors collectively disrupt early myogenesis, emphasizing that prostaglandins alone cannot fully account for the impairment of regenerative processes. Tumor-mediated systemic inflammation may further contribute to impaired satellite cell activation and delayed muscle repair, particularly relevant for injury-prone cachectic patients [50,51].

By composing mimics of cytokines that were found in the CM, we observed significant inhibition with a mixture containing all cytokines, but only on the differentiation of C2C12 cells on day 3. Previously, it was

shown that the inflammatory cytokine TNF α (1 ng/mL or 5 ng/mL) could reduce CK activity [52,53], while insulin-like growth factor 1 (IGF1, 30 ng/mL) increased CK activity [54]. This suggests that TNF α has a direct catabolic effect on skeletal muscle, causing loss of muscle mass, and therefore has an important role in cachectic inflammation [55]. However, these effects have not been validated by exposing muscle cells to similar cytokine levels in cachexia-inducing CM. This was also the case in the study by Hogan et al., which makes it hard to interpret the results of C2C12 incubations with cytokines [17]. In the current study, the concentrations of TNF α in the secretome of the cachexia-inducing cell lines were lower than 0.01 ng/mL, which is at least 100 \times lower compared to what was used in exposure studies in literature. This could explain the modest alterations in CK activity and the short-term inhibitory effect observed in our findings. Importantly, even at these physiologically relevant low levels, tumor secretions transiently suppressed early differentiation, emphasizing that tumor-derived factors can impair muscle regenerative processes at concentrations relevant to cancer patients.

The C26 cell line has been reported to secrete LIF, C-X-C motif chemokine ligand 10 (CXCL10), CCL2, CXCL1 and Oncostatin M (OSM), but not TNF α , myostatin or Interferon gamma (IFNG) [29,56]. Consistent

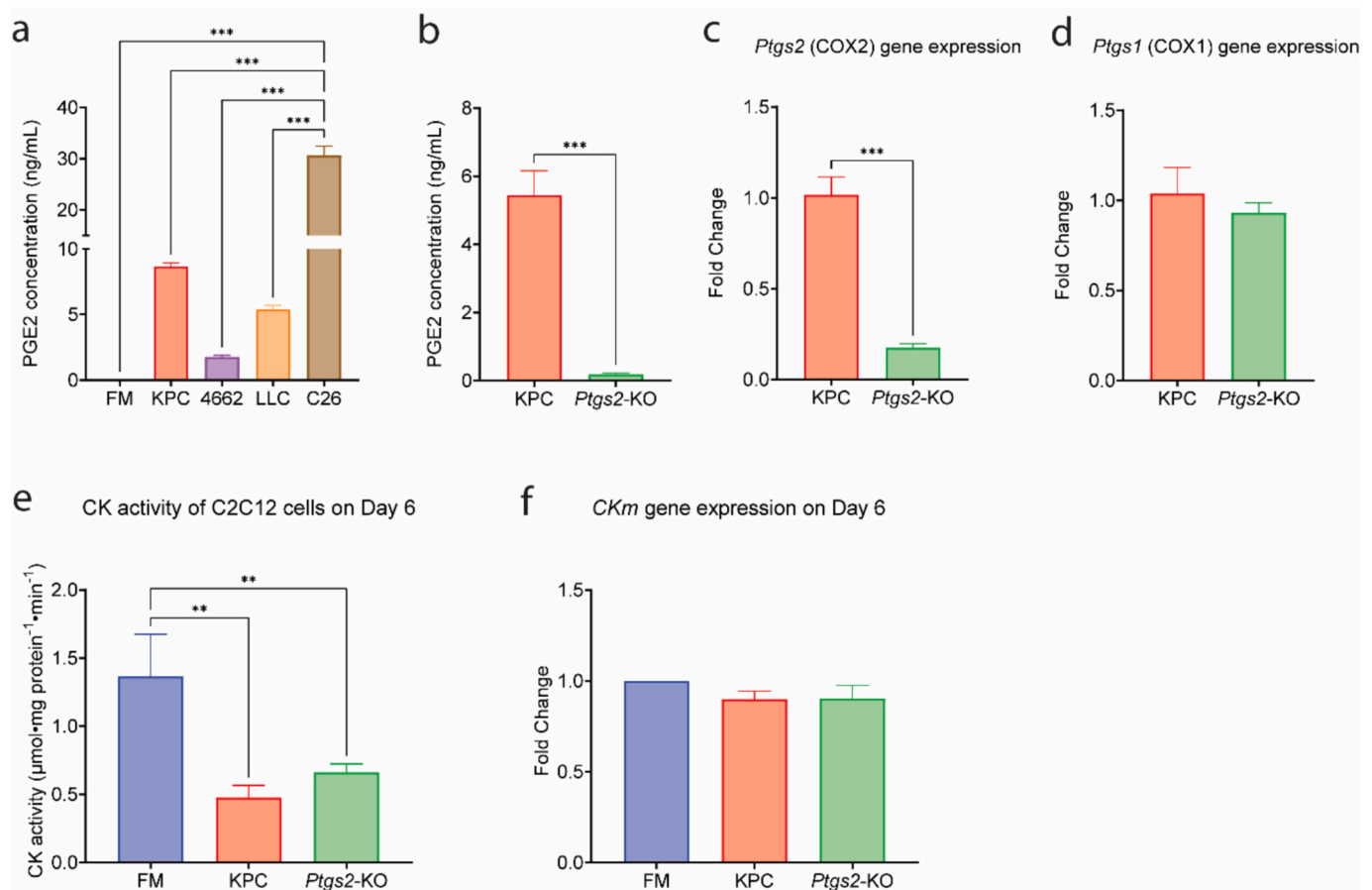


Fig. 5. Validating the role of tumor-derived PGE2 on C2C12 cell differentiation. **a** Prostaglandin E2 concentration in the cachexia-inducing tumor secretomes (KPC, 4662, LLC and C26). **b** Prostaglandin E2 concentration in KPC and *Ptgs2*-KO KPC tumor secretomes. **c** Relative *Ptgs2* (COX2) gene expression, and **d** *Ptgs1* (COX1) gene expression in KPC and *Ptgs2*-KO KPC cells. **e** CK activity and **f** qPCR of *CKm* gene expression in differentiating C2C12 cells exposed to KPC CM and *Ptgs2*-KO KPC CM on day 6. N = 3 (duplicate or triplicate per N). All data were expressed as mean \pm SEM. Data were analyzed by one-way ANOVA with Bonferroni's post hoc test. * $p \leq 0.05$, ** $p \leq 0.01$, *** $p \leq 0.001$, and **** $p \leq 0.0001$.

with previous studies, we detected CXCL10 and CCL2 in our C26 conditioned media (CM), but not TNF α . However, we measured a LIF concentration of 0.011 ng/mL, which is 40-fold lower than the 0.4 ng/mL reported by Seto et al. [29]. For IL6, we found a concentration of 0.026 ng/mL, closely aligning with the 0.028 ng/mL [56] reported by another study, though lower values of 0.007 ng/mL [29] have also been observed. Notably, C26 cells exhibited fewer differentially expressed genes (DEGs) and had a smaller effect on CK activity compared to the KPC, 4662, and LLC cell lines, highlighting the variability between cachexia-inducing models. Our findings also suggest that previously unassociated cytokines, such as CCL20, CXCL5, and PCSK9, may play a role in the tumor secretome, emphasizing the importance of broad profiling tools to identify novel mediators of muscle regenerative impairment.

In addition to the tumor-induced pro-inflammatory cytokines, more tumor factors are likely involved in skeletal muscle wasting during cancer cachexia. For example, recent studies have unveiled the involvement of non-coding RNAs in the development of cancer cachexia. Tumor-derived microvesicles, from both tumor cell lines and patients, were found to induce apoptosis of skeletal muscle cells and primary myoblasts. Specifically, miR-21 and miR-29a secreted by lung and pancreatic tumors promoted atrophy in recipient murine myoblasts by binding to the TLR7/8 receptor and activating the JNK pathway [15]. Moreover, elevated serum miR-203 in colorectal cancer patients posed a risk for myopenia [57]. These findings suggest that non-coding RNAs may further compromise muscle repair, and future studies should investigate the combined effects of cytokines, prostaglandins, and

microRNAs on muscle regenerative processes.

It is important to acknowledge a limitation in our experimental design. Tumor CM were prepared in C2C12 differentiation medium rather than tumor-optimal medium. While this approach ensured compatibility with C2C12 differentiation conditions and avoided confounding effects of growth factors from tumor maintenance medium, it may have resulted in less-than-optimal secretion of tumor factors. Similarly, fresh differentiation medium (FM) was used as the control rather than C2C12-derived CM to avoid potential effects of myokines secreted by C2C12 cells, which could independently influence differentiation [58,59]. Although CM was diluted to restore serum levels, minor nutrient differences cannot be fully excluded. Despite these limitations, the early inhibition of C2C12 differentiation is likely driven by tumor-derived factors, whereas later recovery may reflect nutrient restoration.

In conclusion, our data reveals a significant inhibitory effect of tumor secretions from cachexia-inducing cell lines on myogenesis, reflected by CK activity in C2C12 cells, highlighting the direct impact of cancer on muscle regeneration. This inhibition is accompanied by the upregulation of immune pathways in the exposed C2C12 cells. The variability in secretion profiles across different cell lines emphasizes the need for utilizing multiple cell models in cachexia research. By assessing 14 key factors, our study contributes valuable insights into how tumor-derived factors impair skeletal muscle repair. Overall, these findings highlight the direct impact of tumor secretions on muscle regeneration and offer a foundation for identifying specific mediators and potential therapeutic strategies to support muscle recovery in cachectic patients.

4. Methods

4.1. Cell culture

The mouse colon carcinoma (C26) cell line was kindly obtained from Dr. Donna McCarthy (Ohio State University, USA), and the mouse Lewis lung carcinoma (LLC) cell line was kindly obtained from Dr. Josep Argiles (University of Barcelona, Spain). The mouse myoblast (C2C12) cell line was kindly obtained from Francina Dijk (Nutricia, the Netherlands). The mouse pancreatic ductal adenocarcinoma (PDAC) cell line KPC was provided by Dr. Elizabeth Jaffee [22,60] and the mouse 4662 cell line was generously provided by Robert Vonderheide [61]. The C26 and LLC cells were grown in Dulbecco's Modified Eagle Medium (DMEM, Corning, USA). The KPC and 4662 cells were maintained in low glucose Dulbecco's Modified Eagle Medium (Gibco, ThermoFisher, Waltham, MA). All media were supplemented with 10 % fetal calf serum (FCS, Biowest, USA) and 1 % penicillin-streptomycin (Corning, USA). The C2C12 cells were grown in Dulbecco's Modified Eagle Medium (DMEM, Corning, USA), supplemented with 10 % fetal calf serum (FCS, Biowest, USA) and 1 % penicillin-streptomycin (Corning, USA). The C2C12 cells were differentiated in Dulbecco's Modified Eagle Medium (DMEM, Corning, USA), supplemented with 2 % horse serum (Gibco, ThermoFisher, Waltham, MA) and 1 % penicillin-streptomycin (Corning, USA). All cell lines were incubated at 37 °C in a humidified atmosphere with 5 % CO₂.

4.1.1. CRISPR/Cas9-mediated knockout of *Ptgs2* in KPC cell line

Mouse *Ptgs2* CRISPR/Cas9 knockout plasmid (sc-422,489), *Ptgs2* HDR plasmid (sc-422,489-HDR), control CRISPR/Cas9 Plasmid (sc-418,922), and transfection reagent (sc-395,739) were purchased from Santa Cruz Biotechnology (CA, Heidelberg, Germany). KPC cells were seeded at a density of 7×10^4 in 3 mL of antibiotic-free standard growth medium per well into a six-well plate 24 h prior to transfection. Transfection Reagent was used at a final concentration of 5 % together with a total of 4 µg plasmid (2 µg *Ptgs2* CRISPR/Cas9 KO plasmid with 2 µg *Ptgs2* HDR plasmid) per well. Cells were maintained for 48 h before returning to the growth medium and puromycin selection (20 µg/mL) (sc-108,071). The *Ptgs2* HDR plasmid is designed for the repair of the site-specific Cas9-induced DNA cleavage within the *Ptgs2* gene and contains a puromycin resistance gene to enable selection of stable knockout cells and an RFP gene to visually confirm transfection.

4.1.2. Conditioned medium & immune factor mimics

To make conditioned medium (CM), cells were taken from 90 % confluent flasks and seeded 1:5 (C26 and LLC) and 1:3 (KPC and 4662) in a T75 flask. Cells were allowed to adhere to the flask for two hours in their maintenance medium (GM or GM-LG), thereafter cells were washed twice with phosphate-buffered saline (PBS) and 12 mL of DM-C2C12 was added. All cells were incubated at 37 °C and 5 % CO₂ for 96 h to create CM. After 96 h, CM was harvested and pooled per cell line, centrifuged (5 min at 500g), aliquoted, and stored at -20 °C. The KPC-KO cells were first maintained in low glucose Dulbecco's Modified Eagle Medium (Gibco, ThermoFisher, Waltham, MA) to obtain a confluent layer, and washed twice with PBS prior to seeding in Dulbecco's Modified Eagle Medium (DMEM, Corning, USA), supplemented with 2 % horse serum (Gibco, ThermoFisher, Waltham, MA) and 1 % penicillin-streptomycin (Corning, USA). The cells were incubated at 37 °C and 5 % CO₂ for 72 h to create CM. After 72 h, CM were harvested and pooled, centrifuged (5 min at 500g), aliquoted, and stored at -20 °C.

Mimic medium A, based on the cytokine profiler array (R&D Systems, see below) and luminex ELISA (R&D Systems, see below) consisted of CXCL1, vascular endothelial growth factor (VEGF), C-X-C motif chemokine ligand 16 (CXCL16), serpin E1, C-C motif chemokine ligand 20 (CCL20), proprotein convertase subtilisin/kexin type 9 (PCSK9), IGFBP3 and C-X-C motif chemokine ligand 5 (CXCL5). Mimic medium B, based on IPA upstream regulator analysis (Qiagen, see below) and ELISAs

(R&D Systems, see below), consisted of secreted phosphoprotein 1 (SPP1), IL6, CCL2 and leukemia inhibitory factor (LIF). Mimic medium C contained two prostaglandins, PGE2 and PGF2α. The last mixture, mimic medium D, contained all components of all three mixtures. The concentrations of the inflammatory compounds are provided in Table 1.

4.1.3. C2C12 culture and sample harvest

C2C12 cells were maintained sub-confluent in GM. For the differentiation experiments, cells were seeded in a 24-well plate at 1.14×10^5 cells/mL and 1 mL per well. After 24 h, the medium was changed to differentiation medium (DM), DM with 33 % CM, or DM with an immune factor mixture mimicking CM (Table 1). Fresh medium (FM) refers to unconditioned differentiation medium that had not been exposed to C2C12 cells. To correct for nutrient depletion in CM, a 33 % dilution was performed by mixing CM with FM prior to application to C2C12 cultures. This approach ensured that observed effects were attributable to factors secreted by tumor cells rather than to nutrient depletion or the presence of conditioned medium from differentiating C2C12 cells, which may contain growth factors or other signaling molecules influencing myogenesis. On day 3 and 5 of the differentiation, the medium of all conditions was refreshed. Additionally, on day 3, 5, and 7, samples were harvested for protein and/or RNA isolation (duplicate or triplicate per day). In particular, the medium of the KPC-KO condition was refreshed on day 3 and 6 of the differentiation. Additionally, samples were harvested for RNA isolation on day 6, and harvested for protein on day 3 and 6. Experiments were repeated (N) 3 or 4 times. Cells were washed once with PBS before harvesting. For protein samples, CellLyticM (Sigma, C2978) with added complete, EDTA-free Protease Inhibitor Cocktail (Sigma-Aldrich, 11873580001) was used. Cells were incubated for 15 min on a shaker at RT and homogenized by scraping. Homogenate was centrifuged at 12000g at 4 °C and supernatant was transferred to a

Table 1
Cytokines and prostaglandins used in each mimic.

Mimic medium A	Reference number	Final Conc. (ng/mL) ^{**}
Recombinant Murine CXCL1	Preprotech, 250-11	0.6961
Recombinant Murine VEGF165	Preprotech, 450-32	0.6973
Recombinant Murine CXCL16	Preprotech, 250-28	0.2225
Recombinant mouse Serpin E1	Raybiotech, 230-00730-10	5.453
Recombinant Murine CCL20	Preprotech, 250-27	1.906
Recombinant Mouse PCSK9	R&D Systems, 9258-SE	20.96
Recombinant Mouse IGFBP3	R&D Systems, 775-B3	7.19
Recombinant Murine CXCL5	Preprotech, 250-17	0.9309

Mimic medium B	Reference number	Final Conc. (ng/mL) ^{**}
Prostaglandin E2	R&D Systems, 2296/10	1.305
Prostaglandin F2A	Sanbio, 16010-5	0.906

Mimic medium C	Reference number	Final Conc. (ng/mL) ^{**}
Recombinant Mouse SPP1	R&D Systems, 441-OP-050/CF	122.5
Recombinant Murine IL6	Preprotech, 216-16	0.0012
Recombinant Murine CCL2	Preprotech, 250-10	0.0175
Recombinant Murine LIF	Preprotech, 250-02	0.003

* Mimic medium D, contained all components of all three mixtures.

** This is the final concentration on the cells, e.g. 33 % of the concentration measured in the CM as the CM itself was also applied to the cell at a concentration of 33 %.

clean chilled tube. Protein lysates were stored at -80°C . For the RNA samples, cells were collected with TRIzol Reagent or RLT buffer (Qiagen, 74004) + β -mercaptoethanol. Lysates were homogenized and stored at -20°C .

4.2. Cytokine measurements

The proteome profiler array mouse XL cytokine array kit (R&D Systems, ARY028) was used to measure cytokine levels of the CM samples according to the manufacturer's instructions. Arrays were measured using a ChemiDoc imaging system (Biorad). Analysis of the intensity of the spots was done in Fiji [62] using the DotBlot Analysis. *ijm* macro [63]. Cytokine concentrations were further quantified using the mouse magnetic luminex assay (R&D Systems, LXSAMSM-08) for CCL20, CXCL1, CXCL16, IGFBP-3, CXCL5, PCSK9, Serpin E1 and VEGF according to manufacturer's instructions. CM samples were measured on the MAGPIX System (Luminex Corporation). DuoSet ELISA kits of IL6 (R&D systems, DY406), LIF (R&D systems, DY449), MCP-1/CCL2 (R&D systems, DY479) TNF α (R&D systems, DY410) and Quantikine SPP1 ELISA (R&D systems, MOST00) were performed following manufacturer's instructions.

4.3. Creatine Kinase assay

Protein concentrations were measured using the Pierce BCA Protein Assay Kit (Thermo Fisher Scientific, 23225) following the manufacturer's instructions. Protein lysates were diluted to 0.025 mg/mL using CellLyticM. The reaction mixture (RM, Table 2) and enzyme mixture (EM) were made fresh in every experiment. The chemicals were dissolved in MilliQ water and the pH was set to 7.4 with acetic acid. The EM consisted of 42 μL glucose-6-phosphate dehydrogenase (140 units/mg protein, Sigma, 10127671001) and 34 μL hexokinase (450 units/mg protein, Sigma, 11426362001) dissolved in 1016.88 μL PBS.

To measure creatine kinase (CK), 20 μL sample or blank were pipetted per well in the 96 wells plate and 150 μL of RM was added. Plates were incubated at 37°C for 10 min and 10 μL EM was added. Absorption was measured at 340 nm with a kinetic program for 44 min with an interval of 24 s at 37°C . Between every measurement the plate was shaken for 1 s at medium speed, using the Spectramax M2 (molecular devices). Creatine kinase activity was calculated by using a lag time of 500 s., and V_{max} (absorbance in milli-units per minute) was calculated over 90 points. After subtraction of the background (blank) the following calculation was used: CK activity ($\mu\text{mol}/\text{mg}^{-1}/\text{min}^{-1}$) = (V_{max} x reaction volume in μL) / (6220 (molar absorption coefficient of NADPH at 340 nm) x cm height (= 0.5625 cm for 180 μL volume) x mg protein in the well x 1000 (conversion from milli-OD to OD)).

Table 2
Chemicals used in Creatine Kinase assay reaction mixture.

Chemicals	Reference number	MW	Final conc.	Conc. in RM
			100	
Imidazole	Merck / AM15	68.08	mM	120 mM
Glucose	Sigma / BB05	179.49	20 mM	24 mM
Mg-acetate	Merck / AF17	214.79	10 mM	12 mM
Adenosine diphosphate	Sigma A5285 / FV1	458.15	10 mM	12 mM
Adenosine monophosphate	Sigma A1752 / FV4	415.49	25 mM	30 mM
Nicotinamide adenine dinucleotide phosphate	Sigma N0505 / FV5	828.19	2 mM	2.4 mM
Phosphocreatine	Sigma P7936 / FV6	327.11	35 mM	42 mM
	Sigma A9165 / CK2.02	163.66	20 mM	24 mM
Acetyl-cysteine	Sigma D4022 / stock 10 mg/mL in PBS	915.5	10 μM	12 μM

4.4. Quantitative PCR

The C2C12 cell samples were collected in TRIzol (Invitrogen). Total RNA was isolated using the RNeasy Micro kit from Qiagen (Venlo, the Netherlands). Subsequently, 500 ng of RNA was used to synthesize complementary DNA using the iScript cDNA Synthesis kit (Bio-Rad Laboratories, Veenendaal, The Netherlands). mRNA levels of various genes were determined by reverse transcription-quantitative PCR using SensiMix (Bioline; GC Biotech, Alphen aan den Rijn, The Netherlands) on a CFX384 real-time PCR detection system (Bio-Rad Laboratories). Primer sets for *Rplp0/36B4*, *Tbp*, *CKm*, *Ptgs2*, and *Ptgs1* were used (Table 3). *Rplp0* and *Tbp* were used as housekeeping genes of *CKm*. *Rplp0* was used as the housekeeping gene of *Ptgs2* and *Ptgs1*. Primers were synthesized by Eurogentec (Seraing, Belgium).

4.5. Transcriptome analysis

TRIzol C2C12 samples were used for sequencing. Samples were thawed and 0.2 mL chloroform per 1 mL of TRIzol was added and incubated for 2–3 min. Samples were centrifuged for 15 min at 12000g at 4°C and the aqueous phase was transferred to a new tube. From this aqueous phase, the RNA was isolated using RNeasy Micro Kit (Qiagen, 74004) following the manufacturer's instructions. RNA was eluted in 14 μL RNase-free water and RNA yield was determined by nanodrop. RNA quality was determined using the Bioanalyzer (Agilent) and the RNA 6000 Nano Kit (Agilent, 5067–1511). Technical triplicates were pooled, resulting in a total of three biological replicates per condition. All samples were diluted to a concentration of 40 ng/ μL and shipped in dry ice to BGI Tech Solutions (Hong Kong). At BGI tech solutions, DNaseq eukaryotic transcriptome re-sequencing (strand-specific) was done by applying at least 20 M clean reads per sample. Filtered sequencing reads were collected (6–9 GB data per sample).

The analysis of the data was done on the high-performance computer infrastructure hosted by Wageningen University & Research. Quality control was done using FastQC [64], and next, alignment was done using STAR [65]. Reads were counted using HTSeq [66] and files were exported to do further analysis using R studio [67]. DESeq2 [68] was used to detect differentially expressed genes (DEGs), and *P*-values were adjusted for multiple testing by the Benjamini-Hochberg false discovery rate (FDR) procedure [69]. An adjusted *p*-value (or FDR) of $p < 0.05$ was considered significantly regulated. Venn diagrams and scatter plots were made using the R libraries ggplot2 [70] and VennDiagram [71]. Changes in individual genes were related to changes in pathways by gene set enrichment analysis (GSEA) [72], analysis and visualization were performed using the package clusterProfiler [73] and DOSE [74]. Analysis was done for Biological Process (BP) gene ontology (GO) terms and only gene sets consisting of more than 50 and fewer than 1000 genes were considered. For each comparison, genes were ranked on their GeneRatio (the number of genes of the input list associated with the given GO term / the total number of input genes). Additionally, data were analyzed through the use of Ingenuity Pathway Analysis (IPA). Upstream analysis was used to identify possible (cytokine) regulators, only cytokines were considered when they had a activation *z*-score > 2 and fold change > 0.9 . Additionally, all regulators that were flagged with 'bias' were removed from the analysis. These RNA-seq data are available at the GEO under the accession number GEO: GSE194370.

4.6. Statistics

All statistical analyses were performed in GraphPad Prism 9.5.1 software or R and R studio [67]. Quantitative data are reported as mean \pm standard error. Two-tailed Students *t*-tests were performed when comparing two groups. When comparing more than two groups of a single genotype, One-way ANOVA was utilized. Correlation analyses were performed after the assessment of normality using Shapiro–Wilk tests, demonstrating that all data analyzed followed a Gaussian

Table 3
Primers used for qPCR.

Gene	Name	Forward	Reverse
Tbp	TATA-box binding protein	CAGTGCCAGCATCACTATTTC	TGGAAGGCTGTTGTTCTGGT
Rplp0/36B4	Ribosomal protein lateral stalk subunit P0	ATGGGTACAAGCGCGTCCTG	GCCTTGACCTTTTCAGTAAG
CKm	Creatine kinase muscle	GGCCTGCAGAAGATTGAGGA	CTTGGGGTGTCTTGCTCAGGT
Ptgs2	Prostaglandin-Endoperoxide Synthase 2	TGAGCAACTATTTCCAAACCAGC	GCACGTAGTCTTCGATCACTATC
Ptgs1	Prostaglandin-Endoperoxide Synthase 1	GAATGCCACTTCATCCGAGAAG	GCTCACATTGGAGAAGACTCC

distribution (Pearson correlation, parametric data). Two-way ANOVA with Bonferroni multiple comparisons test was utilized when comparing multiple genotypes and treatment groups. For all analyses, a *P*-value of <0.05 was considered to be statistically significant.

CRedit authorship contribution statement

Miranda van der Ende: Writing – original draft, Formal analysis, Data curation, Conceptualization. **Xiaolin Li:** Writing – review & editing, Writing – original draft, Visualization, Software, Formal analysis, Data curation. **Mieke Poland:** Writing – review & editing, Resources, Methodology. **Fleur Jansen:** Writing – review & editing, Formal analysis, Data curation. **Jocelijn Meijerink:** Writing – review & editing, Conceptualization. **Jaap Keijer:** Writing – review & editing, Supervision. **Renger F. Witkamp:** Writing – review & editing, Supervision, Project administration. **Sander Grefte:** Writing – review & editing, Supervision, Project administration, Funding acquisition, Formal analysis, Conceptualization. **Klaske van Norren:** Writing – review & editing, Supervision, Project administration, Funding acquisition, Conceptualization.

Declaration of competing interest

The authors declare that they have no known competing financial interests or personal relationships that could have appeared to influence the work reported in this paper.

Acknowledgments

The authors would like to thank Bart Lagerwaard, Jenny Jansen and Guido Hooiveld for their practical help and tips during this study. Additionally, we would like to thank Donna McCarthy (Ohio State University, USA) for the C26 cell line, Josep Argiles (University of Barcelona, Spain) for the LLC cell line, Francina Dijk (Nutricia, the Netherlands) for the C2C12 cell line and Elizabeth Jaffee and Daniel Marks (Oregon Health and Science University, USA) for the KPC and the genetic variation KPC-4662 cell lines. Also, we would like to thank Francina Dijk, Veerle Ottenheim, and Yukako Tokutake for their help with the protocol for the CK assay.

Appendix A. Supplementary data

Supplementary data to this article can be found online at <https://doi.org/10.1016/j.bbamcr.2025.120093>.

Data availability

Data will be made available on request.

References

- [1] K. Fearon, F. Strasser, S.D. Anker, I. Bosaeus, E. Bruera, R.L. Fainsinger, A. Jatoi, C. Loprinzi, N. MacDonald, G. Mantovani, M. Davis, M. Muscaritoli, F. Ottery, L. Radbruch, P. Ravasco, D. Walsh, A. Wilcock, S. Kaasa, V.E. Baracos, Definition and classification of cancer cachexia: an international consensus, *Lancet Oncol.* 12 (2011) 489–495, [https://doi.org/10.1016/S1470-2045\(10\)70218-7](https://doi.org/10.1016/S1470-2045(10)70218-7).
- [2] L. Martin, T. Reiman, R.A. Murphy, S. Ghosh, Cancer cachexia in the age of obesity: skeletal muscle depletion is a powerful prognostic factor, independent of body mass index circulating and tissue fatty acid biomarkers and cardiometabolic outcomes view project international audit of nutrition care in patients with foregut tumors (INFORM) view project, *J. Clin. Oncol.* (2013), <https://doi.org/10.1200/JCO.2012.45.2722>.
- [3] M. Shibata, M. Fukahori, E. Kasamatsu, K. Machii, S. Hamauchi, A retrospective cohort study to investigate the incidence of cachexia during chemotherapy in patients with colorectal cancer, *Adv. Ther.* 37 (2020) 5010–5022, <https://doi.org/10.1007/S12325-020-01516-6/TABLES/4>.
- [4] O.M. Vagnildhaug, T.R. Balstad, S.S. Almberg, C. Brunelli, A.K. Knudsen, S. Kaasa, M. Thronæs, B. Laird, T.S. Solheim, A cross-sectional study examining the prevalence of cachexia and areas of unmet need in patients with cancer, *Support Care Cancer* 26 (2018) 1871–1880, <https://doi.org/10.1007/S00520-017-4022-Z/TABLES/4>.
- [5] L.G. Melstrom, K.A. Melstrom Jr., X.Z. Ding, T.E. Adrian, Mechanisms of skeletal muscle degradation and its therapy in cancer cachexia, *Histol. Histopathol.* 22 (7) (2007) 805–814, <https://doi.org/10.14670/HH-22.805> (accessed August 31, 2023), <https://digitum.um.es/digitum/handle/10201/27602>.
- [6] M.S. Anker, R. Holcomb, M. Muscaritoli, S. von Haehling, W. Haverkamp, A. Jatoi, J.E. Morley, F. Strasser, U. Landmesser, A.J.S. Coats, S.D. Anker, Orphan disease status of cancer cachexia in the USA and in the European Union: a systematic review, *J. Cachexia. Sarcopenia Muscle* 10 (2019) 22–34, <https://doi.org/10.1002/JCSM.12402>.
- [7] J. Ni, L. Zhang, Cancer cachexia: definition, staging, and emerging treatments, *Cancer Manag. Res.* 12 (2020) 5597–5605, <https://doi.org/10.2147/CMAR.S261585>.
- [8] M. van der Ende, S. Grefte, R. Plas, J. Meijerink, R.F. Witkamp, J. Keijer, K. van Norren, Mitochondrial dynamics in cancer-induced cachexia, *Biochim. Biophys. Acta (BBA) – Rev. Cancer* 1870 (2018) 137–150, <https://doi.org/10.1016/J.BBRCAN.2018.07.008>.
- [9] F. Marchildon, É. Lamarche, N. Lala-Tabbert, C. St-Louis, N. Wiper-Bergeron, Expression of CCAAT/enhancer binding protein Beta in muscle satellite cells inhibits Myogenesis in Cancer Cachexia, *PLoS One* 10 (2015) e0145583, <https://doi.org/10.1371/JOURNAL.PONE.0145583>.
- [10] S. Inaba, A. Hinohara, M. Tachibana, K. Tsujikawa, S. Fukada, Muscle regeneration is disrupted by cancer cachexia without loss of muscle stem cell potential, *PLoS One* 13 (2018) e0205467, <https://doi.org/10.1371/JOURNAL.PONE.0205467>.
- [11] P.C. Arneson, J.D. Doles, Impaired muscle regeneration in cancer-associated cachexia, *Trends Cancer* 5 (2019) 579–582, <https://doi.org/10.1016/J.TRECAN.2019.07.010>.
- [12] E.E. Talbert, D.C. Guttridge, Impaired regeneration: a role for the muscle microenvironment in cancer cachexia, *Semin. Cell Dev. Biol.* 54 (2016) 82–91, <https://doi.org/10.1016/J.SEMCDB.2015.09.009>.
- [13] N. Bakkar, D.C. Guttridge, NF-κB signaling: a tale of two pathways in skeletal myogenesis 90 (2010) 495–511, <https://doi.org/10.1152/PHYSREV.00040.2009>, doi:10.1152/PHYSREV.00040.2009.
- [14] W.A. He, E. Berardi, V.M. Cardillo, S. Acharyya, P. Aulino, J. Thomas-Ahner, J. Wang, M. Bloomston, P. Muscarella, P. Nau, N. Shah, M.E.R. Butchbach, K. Ladner, S. Adamo, M.A. Rudnicki, C. Keller, D. Coletti, F. Montanaro, D. C. Guttridge, NF-κB-mediated Pax7 dysregulation in the muscle microenvironment promotes cancer cachexia, *J. Clin. Invest.* 123 (2013) 4821–4835, <https://doi.org/10.1172/JCI68523>.
- [15] W.A. He, F. Calore, P. Londhe, A. Canella, D.C. Guttridge, C.M. Croce, Microvesicles containing miRNAs promote muscle cell death in cancer cachexia via TLR7, *Proc. Natl. Acad. Sci. USA* 111 (2014) 4525–4529, <https://doi.org/10.1073/PNAS.1402714111;WEBSITE=WEBSITE:PNAS-SITE;ISSUE=ISSUE:DOI>.
- [16] E.E. Talbert, H.L. Lewis, M.R. Farren, M.L. Ramsey, J.M. Chakedis, P. Rajasekera, E. Haverick, A. Sarna, M. Bloomston, T.M. Pawlik, T.A. Zimmers, G.B. Lesinski, P. A. Hart, M.E. Dillhoff, C.R. Schmidt, D.C. Guttridge, Circulating monocyte chemoattractant protein-1 (MCP-1) is associated with cachexia in treatment-naïve pancreatic cancer patients, *J. Cachexia. Sarcopenia Muscle* 9 (2018) 358–368, <https://doi.org/10.1002/JCSM.12251>.
- [17] K.A. Hogan, D.S. Cho, P.C. Arneson, A. Samani, P. Palines, Y. Yang, J.D. Doles, Tumor-derived cytokines impair myogenesis and alter the skeletal muscle immune microenvironment, *Cytokine* 107 (2018) 9–17, <https://doi.org/10.1016/J.CYTO.2017.11.006>.
- [18] X.Y. Huang, Z.L. Huang, J.H. Yang, Y.H. Xu, J.S. Sun, Q. Zheng, C. Wei, W. Song, Z. Yuan, Pancreatic cancer cell-derived IGFBP-3 contributes to muscle wasting, *J. Exp. Clin. Cancer Res.* 35 (2016) 1–13, <https://doi.org/10.1186/S13046-016-0317-Z/FIGURES/6>.
- [19] M. Nakanishi, D.W. Rosenberg, Multifaceted roles of PGE2 in inflammation and cancer, *Semin. Immunopathol.* 35 (2) (2012) 123–137, <https://doi.org/10.1007/S00281-012-0342-8>.
- [20] R.A. Standley, S.Z. Liu, B. Jemiolo, S.W. Trappe, T.A. Trappe, Prostaglandin E2 induces transcription of skeletal muscle mass regulators interleukin-6 and muscle

- RING finger-1 in humans, Prostaglandins Leukot. Essent. Fat. Acids 88 (2013) 361–364, <https://doi.org/10.1016/j.plefa.2013.02.004>.
- [21] V. Horsley, G.K. Pavlath, Prostaglandin F_{2α} stimulates growth of skeletal muscle cells via an NFATC2-dependent pathway, J. Cell Biol. 161 (2003) 111–118, <https://doi.org/10.1083/JCB.200208085>.
- [22] K.A. Michaelis, X. Zhu, K.G. Burfeind, S.M. Krasnow, P.R. Levasseur, T.K. Morgan, D.L. Marks, Establishment and characterization of a novel murine model of pancreatic cancer cachexia, J. Cachexia. Sarcopenia Muscle 8 (2017) 824–838, <https://doi.org/10.1002/JCSM.12225>.
- [23] R.A. Evans, M.S. Diamond, A.J. Rech, T. Chao, M.W. Richardson, J.H. Lin, D. L. Bajor, K.T. Byrne, B.Z. Stanger, J.L. Riley, N. Markosyan, R. Winograd, R. H. Vonderheide, Lack of immunoeating in murine pancreatic cancer reversed with neointigen, JCI Insight 1 (2016) 88328, <https://doi.org/10.1172/JCI.INSIGHT.88328>.
- [24] G. Wang, H. Zhang, D. Lyden, Tumour-regulated anorexia preceding cachexia, Nat. Cell Biol. 23 (2) (2021) 111–113, <https://doi.org/10.1038/s41556-021-00635-8>.
- [25] A. Bonetto, J.E. Rupert, R. Barreto, T.A. Zimmers, The colon-26 carcinoma tumor-bearing mouse as a model for the study of cancer cachexia, JoVE (J. Vis. Exp.) (2016) e54893, <https://doi.org/10.3791/54893>.
- [26] J.S. Chamberlain, J.B. Jaynes, D.D. Hauschka Stephen, Regulation of creatine kinase induction in differentiating mouse myoblasts, Doi:10.1128/Mcb.5.3.484-492.1985 5 (2023) 484–492, <https://doi.org/10.1128/MCB.5.3.484-492.1985>.
- [27] X. Li, T. Holtrop, F.A.C. Jansen, B. Olson, P. Levasseur, X. Zhu, M. Poland, W. Schalmwijk, R.F. Witkamp, D.L. Marks, K. van Norren, Lipopolysaccharide-induced hypothalamic inflammation in cancer cachexia-anorexia is amplified by tumour-derived prostaglandin E₂, J. Cachexia. Sarcopenia Muscle 13 (2022) 3014–3027, <https://doi.org/10.1002/JCSM.13093>.
- [28] A.E. Tuomisto, M.J. Mäkinen, J.P. Väyrynen, Systemic inflammation in colorectal cancer: underlying factors, effects, and prognostic significance, World J. Gastroenterol. 25 (2019) 4383, <https://doi.org/10.3748/WJG.V25.I3.4383>.
- [29] D.N. Seto, S.C. Kandarian, R.W. Jackman, A key role for leukemia inhibitory factor in C26 Cancer Cachexia, J. Biol. Chem. 290 (2015) 19976–19986, <https://doi.org/10.1074/JBC.M115.638411>.
- [30] F. Pin, L.J. Novinger, J.R. Huot, R.A. Harris, M.E. Couch, T.M. O'Connell, A. Bonetto, PDK4 drives metabolic alterations and muscle atrophy in cancer cachexia, FASEB J. 33 (2019) 7778–7790, <https://doi.org/10.1096/FJ.201802799R>.
- [31] R.W. Jackman, J. Floro, R. Yoshimine, B. Zitin, M. Eiampikul, K. El-Jack, D.N. Seto, S.C. Kandarian, Continuous release of tumor-derived factors improves the modeling of cachexia in muscle cell culture, Front. Physiol. 8 (2017) 297065, <https://doi.org/10.3389/fphys.2017.00738/BIBTEX>.
- [32] K.A.S. Silva, J. Dong, Y. Dong, Y. Dong, N. Schor, D.J. Tweardy, L. Zhang, W. E. Mitch, Inhibition of Stat3 activation suppresses Caspase-3 and the ubiquitin-proteasome system, leading to preservation of muscle mass in Cancer Cachexia, J. Biol. Chem. 290 (2015) 11177–11187, <https://doi.org/10.1074/JBC.M115.641514>.
- [33] R. Sun, S. Zhang, W. Hu, X. Lu, N. Lou, Z. Yang, S. Chen, X. Zhang, H. Yang, Valproic acid attenuates skeletal muscle wasting by inhibiting C/EBPβ-regulated atrogen1 expression in cancer cachexia, Am. J. Physiol. Cell Physiol. 311 (2016) C101–C115, <https://doi.org/10.1152/AJPCELL.00344.2015/ASSET/IMAGES/LARGE/ZH00111679540009.JPEG>.
- [34] K.R. Bohnert, P. Goli, A. Roy, A.K. Sharma, G. Xiong, Y.S. Gallot, A. Kumar, The toll-like receptor/MyD88/XBP1 signaling axis mediates skeletal muscle wasting during cancer cachexia, Mol. Cell. Biol. 39 (2019), https://doi.org/10.1128/MCB.00184-19/SUPPL_FILE/TMCB_A_12276991_SM0001.PDF.
- [35] E. Wyart, S. Reano, M.Y. Hsu, D.L. Longo, M. Li, E. Hirsch, N. Filigheddu, A. Ghigo, C. Riganti, P.E. Porporato, Metabolic alterations in a slow-paced model of pancreatic cancer-induced wasting, Oxidative Med. Cell. Longev. 2018 (2018), <https://doi.org/10.1155/2018/6419805>.
- [36] J.E. Rupert, A. Narasimhan, D.H.A. Jengelly, Y. Jiang, J. Liu, E. Au, L. M. Silverman, G. Sandusky, A. Bonetto, S. Cao, X. Lu, T.M. O'Connell, Y. Liu, L. G. Koniaris, T.A. Zimmers, Tumor-derived IL-6 and trans-signaling among tumor, fat, and muscle mediate pancreatic cancer cachexia, J. Exp. Med. 218 (2021), <https://doi.org/10.1084/JEM.20190450/211985>.
- [37] A.P. Duval, C. Jeanneret, T. Santoro, O. Dormond, mTOR and Tumor Cachexia, Int. J. Mol. Sci. 19 (2018) 2225, <https://doi.org/10.3390/IJMS19082225>.
- [38] D. Costamagna, P. Costelli, M. Sampaolesi, F. Penna, Role of inflammation in muscle homeostasis and Myogenesis, Mediat. Inflamm. 2015 (2015), <https://doi.org/10.1155/2015/805172>.
- [39] D.C. Guttridge, M.W. Mayo, L.V. Madrid, C.Y. Wang, J. Baldwin, NF-κB-induced loss of MyoD messenger RNA: possible role in muscle decay and cachexia, Science (1979) 289 (2000) 2363–2365, https://doi.org/10.1126/SCIENCE.289.5488.2363/SUPPL_FILE/1052671SL_THUMB.GIF.
- [40] G.P. Marceca, G. Nigita, F. Calore, C.M. Croce, MicroRNAs in skeletal muscle and hints on their potential role in muscle wasting during Cancer Cachexia, Front. Oncol. 10 (2020) 607196, <https://doi.org/10.3389/FONC.2020.607196/BIBTEX>.
- [41] C.R. Bell, S. Zelenay, COX-2 upregulation by tumour cells post-chemotherapy fuels the immune evasive dark side of cancer inflammation, Cell Stress 6 (2022) 76, <https://doi.org/10.15698/CST2022.09.271>.
- [42] D. Wang, R.N. Dubois, Prostaglandins and CANCER, Gut 55 (2006) 115–122, <https://doi.org/10.1136/GUT.2004.047100>.
- [43] B. Rigas, I.S. Goldman, L. Levine, Altered eicosanoid levels in human colon cancer, J. Lab. Clin. Med. 122 (1993) 518–523, <https://doi.org/10.5555/URI:PII:002221439390010V>.
- [44] V. Karpishev, A. Nikkhoo, M. Hojjat-Farsangi, A. Namdar, G. Azizi, G. Ghalamfarsa, G. Sabz, M. Yousefi, B. Yousefi, F. Jadidi-Niaragh, Prostaglandin E₂ as a potent therapeutic target for treatment of colon cancer, Prostaglandins Other Lipid Mediat. 144 (2019) 106338, <https://doi.org/10.1016/J.PROSTAGLANDINS.2019.106338>.
- [45] PGE₂ produced by lung Cancer suppresses immune function through T-regulatory cells and can be blocked by the COX2 inhibitor Celebrex, Cancer Biol. Ther. 4 (2005), <https://doi.org/10.4161/CBT.4.8.2034>.
- [46] S. Hasan, M. Satake, D.W. Dawson, H. Funahashi, E. Angst, V.L.W. Go, H.A. Reber, O.J. Hines, G. Eibl, Expression analysis of the prostaglandin E₂ production pathway in human pancreatic cancers, Pancreas 37 (2008) 121–127, <https://doi.org/10.1097/MPA.0B013E31816618BA>.
- [47] C. Charo, V. Holla, T. Arumugam, R. Hwang, P. Yang, R.N. Dubois, D.G. Menter, C. D. Logsdon, V. Ramachandran, Prostaglandin E₂ regulates pancreatic stellate cell activity via the EP4 receptor, Pancreas 42 (2013) 467–474, <https://doi.org/10.1097/MPA.0B013E318264D0F8>.
- [48] S.Z. Liu, B. Jemiolo, K.M. Lavin, B.E. Lester, S.W. Trappe, T.A. Trappe, Prostaglandin E₂/cyclooxygenase pathway in human skeletal muscle: influence of muscle fiber type and age, J. Appl. Physiol. 120 (2016) 546–551, <https://doi.org/10.1152/JAPPLPHYSIOL.00396.2015/ASSET/IMAGES/LARGE/ZDG0021616910004.JPEG>.
- [49] J.F. Markworth, D. Cameron-Smith, Prostaglandin F_{2α} stimulates PI3K/ERK/mTOR signaling and skeletal myotube hypertrophy, Am. J. Physiol. Cell Physiol. 300 (2011) 671–682, <https://doi.org/10.1152/AJPCELL.00549.2009/ASSET/IMAGES/LARGE/ZH00031165540007.JPEG>.
- [50] B. Seruga, H. Zhang, L.J. Bernstein, I.F. Tannock, Cytokines and their relationship to the symptoms and outcome of cancer, Nat. Rev. Cancer 8 (11) (2008) 887–899, <https://doi.org/10.1038/nrc2507>.
- [51] B.H.L. Tan, J.A. Ross, S. Kaasa, F. Skorpen, K.C.H. Fearon, Identification of possible genetic polymorphisms involved in cancer cachexia: a systematic review, J. Genet. 90 (2011) 165–177, <https://doi.org/10.1007/S12041-011-0027-4/METRICS>.
- [52] R.C.J. Langen, A.M.W.J. Schols, M.C.J.M. Kelders, E.F.M. Wouters, Y.M. W. Janssen-Heininger, Inflammatory cytokines inhibit myogenic differentiation through activation of nuclear factor-κB, FASEB J. 15 (2001) 1169–1180, <https://doi.org/10.1096/FJ.00-0463>.
- [53] L. Fernández-Celemín, N. Pasko, V. Blomart, J.P. Thissen, Inhibition of muscle insulin-like growth factor I expression by tumor necrosis factor-α, Am. J. Physiol. Endocrinol. Metab. 283 (2002) <https://doi.org/10.1152/AJPCENDO.00054.2002/ASSET/IMAGES/LARGE/H11121026012.JPEG>.
- [54] S. Sawano, K. Baba, Y. Sonoda, J. ichiro Wakamatsu, S. Tomonaga, M. Furuse, Y. Sato, R. Tatsumi, Y. Ikeuchi, W. Mizunoya, Beef extract supplementation promotes myoblast proliferation and myotube growth in C2C12 cells, Eur. J. Nutr. 59 (2020) 3735–3743, <https://doi.org/10.1007/S00394-020-02205-4/FIGURES/4>.
- [55] H.J. Patel, B.M. Patel, TNF-α and cancer cachexia: molecular insights and clinical implications, Life Sci. 170 (2017) 56–63, <https://doi.org/10.1016/J.LFS.2016.11.033>.
- [56] S.C. Kandarian, R.L. Nosacka, A.E. Delitto, A.R. Judge, S.M. Judge, J.D. Ganey, J. D. Moreira, R.W. Jackman, Tumor-derived leukaemia inhibitory factor is a major driver of cancer cachexia and morbidity in C26 tumour-bearing mice, J. Cachexia. Sarcopenia Muscle 9 (2018) 1109–1120, <https://doi.org/10.1002/JCSM.12346>.
- [57] Y. Okugawa, Y. Toiyama, K. Hur, A. Yamamoto, C. Yin, S. Ide, T. Kitajima, H. Fujikawa, H. Yasuda, Y. Koike, Y. Okita, J. Hiro, S. Yoshiyama, T. Araki, C. Miki, D.C. McMillan, A. Goel, M. Kusunoki, Circulating miR-203 derived from metastatic tissues promotes myopenia in colorectal cancer patients, J. Cachexia. Sarcopenia Muscle 10 (2019) 536–548, <https://doi.org/10.1002/JCSM.12403>.
- [58] P. Ni, L. Yang, F. Li, Exercise-derived skeletal myogenic exosomes as mediators of intercellular crosstalk: a major player in health, disease, and exercise, J. Physiol. Biochem. 79 (2023) 501–510, <https://doi.org/10.1007/S13105-023-00969-X/FIGURES/2>.
- [59] X. Chen, Y. Zhang, Z. Deng, C. Song, L. Yang, R. Zhang, P. Zhang, Y. Xiu, Y. Su, J. Luo, J. Xu, H. Dai, Keratocan improves muscle wasting in sarcopenia by promoting skeletal muscle development and fast-twitch fibre synthesis, J. Cachexia. Sarcopenia Muscle 16 (2025) e13724, <https://doi.org/10.1002/JCSM.13724>.
- [60] B.P. Keenan, Y. Saenger, M.I. Kafrouni, A. Leubner, P. Lauer, A. Maitra, A.A. Rucki, A.J. Gunderson, L.M. Coussens, D.G. Brockstedt, T.W. Dubensky, R. Hassan, T. D. Armstrong, E.M. Jaffee, A Listeria vaccine and depletion of T-regulatory cells activate immunity against early stage pancreatic intraepithelial neoplasms and prolong survival of mice, Gastroenterology 146 (2014) 1784–1794.e6, <https://doi.org/10.1053/J.GASTRO.2014.02.055>.
- [61] C. Twyman-Saint Victor, A.J. Rech, A. Maity, R. Rengan, K.E. Pauken, E. Stelekati, J.L. Benci, B. Xu, H. Dada, P.M. Odorizzi, R.S. Herati, K.D. Mansfield, D. Patsch, R. K. Amaravadi, L.M. Schuchter, H. Ishwaran, R. Mick, D.A. Pryma, X. Xu, M. D. Feldman, T.C. Gangadhar, S.M. Hahn, E.J. Wherry, R.H. Vonderheide, A. J. Minn, Radiation and dual checkpoint blockade activate non-redundant immune mechanisms in cancer, Nature 520 (7547) (2015) 373–377, <https://doi.org/10.1038/nature14292>.
- [62] J. Schindelin, I. Arganda-Carreras, E. Frise, V. Kaynig, M. Longair, T. Pietzsch, S. Preibisch, C. Rueden, S. Saalfeld, B. Schmid, J.Y. Tinevez, D.J. White, V. Hartenstein, K. Eliceiri, P. Tomancak, A. Cardona, et al., Nat. Methods 9 (7) (2012) 676–682, <https://doi.org/10.1038/nmeth.2019>.
- [63] GitHub - ahklemm/AnalyzeDotBlots: ImageJ macro script to measure intensities in dot blots in e.g. protein arrays. <https://github.com/ahklemm/AnalyzeDotBlots>, 2020. (Accessed 6 November 2023).
- [64] Babraham Bioinformatics - FastQC A Quality Control tool for High Throughput Sequence Data. <https://www.bioinformatics.babraham.ac.uk/projects/fastqc/>, 2019. (Accessed 6 November 2023).

- [65] A. Dobin, C.A. Davis, F. Schlesinger, J. Drenkow, C. Zaleski, S. Jha, P. Batut, M. Chaisson, T.R. Gingeras, STAR: ultrafast universal RNA-seq aligner, *Bioinformatics* 29 (2013) 15–21, <https://doi.org/10.1093/BIOINFORMATICS/BTS635>.
- [66] S. Anders, P.T. Pyl, W. Huber, HTSeq—a Python framework to work with high-throughput sequencing data, *Bioinformatics* 31 (2015) 166–169, <https://doi.org/10.1093/BIOINFORMATICS/BTU638>.
- [67] R.M. Baldwin, K. Owzar, H. Zembutsu, A. Chhibber, M. Kubo, C. Jiang, D. Watson, R.J. Eclow, J. Mefford, H.L. McLeod, P.N. Friedman, C.A. Hudis, E.P. Winer, E. M. Jorgenson, J.S. Witte, L.N. Shulman, Y. Nakamura, M.J. Ratain, D.L. Kroetz, R: A language and environment for statistical computing, (no title) 18 (2010) 5099–5109, <https://doi.org/10.1158/1078-0432.CCR-12-1590>.
- [68] M.I. Love, W. Huber, S. Anders, Moderated estimation of fold change and dispersion for RNA-seq data with DESeq2, *Genome Biol.* 15 (2014) 1–21, <https://doi.org/10.1186/S13059-014-0550-8/FIGURES/9>.
- [69] Y. Benjamini, Y. Hochberg, Controlling the false discovery rate: a practical and powerful approach to multiple testing, *J. R. Stat. Soc. B Methodol.* 57 (1995) 289–300, <https://doi.org/10.1111/J.2517-6161.1995.TB02031.X>.
- [70] H. Wickham, *Data Analysis*, 2016, pp. 189–201, https://doi.org/10.1007/978-3-319-24277-4_9.
- [71] H. Chen, P.C. Boutros, VennDiagram: a package for the generation of highly-customizable Venn and Euler diagrams in R, *BMC Bioinformatics* 12 (2011) 1–7, <https://doi.org/10.1186/1471-2105-12-35/TABLES/1>.
- [72] A. Subramanian, P. Tamayo, V.K. Mootha, S. Mukherjee, B.L. Ebert, M.A. Gillette, A. Paulovich, S.L. Pomeroy, T.R. Golub, E.S. Lander, J.P. Mesirov, Gene set enrichment analysis: a knowledge-based approach for interpreting genome-wide expression profiles, *Proc. Natl. Acad. Sci. USA* 102 (2005) 15545–15550, https://doi.org/10.1073/PNAS.0506580102/SUPPL_FILE/06580FIG7.JPG.
- [73] G. Yu, L.G. Wang, Y. Han, Q.Y. He, ClusterProfiler: an R package for comparing biological themes among gene clusters, *OMICS* 16 (2012) 284–287, <https://doi.org/10.1089/omi.2011.0118>.
- [74] G. Yu, L.G. Wang, G.R. Yan, Q.Y. He, DOSE: an R/Bioconductor package for disease ontology semantic and enrichment analysis, *Bioinformatics* 31 (2015) 608–609, <https://doi.org/10.1093/BIOINFORMATICS/BTU684>.